Electronic Supporting Information

Double complex salts based on tetraamminplatinum(II) and vanadyl(IV) bisoxalate for the preparation of bimetallic Pt-V alloy

Sofia N. Vorobyeva,*[a] Zakhar V.Rudzis, [a,b] Taisiya S. Sukhikh,[a] Evgeny Yu. Filatov,[a] Pavel E. Plusnin, [a] Vladimir A. Nadolinny,[a] Artem S. Bogomyakov, [c] and Sergey V. Korenev[a]

a. *Nikolaev Institute of Inorganic Chemistry, Siberian Branch of Russian Academy of Sciences, 3, Acad. Lavrentiev Ave., Novosibirsk 630090, Russia. E-mail: vorobyeva@niic.nsc.ru(Sofiya N.Vorobyeva)*

b. *Novosibirsk State University, 1, Pirogova str., Novosibirsk 630090, Russia .*

c. *International Tomography Center, SB RAS, Institutskaya str., 3a, Novosibirsk, Russian Federation.*

Table of Contents

Table S1. Crystal data and structure refinement for **$(Bu_4N)_2[VO(C_2O_4)_2]$ (I)**, **$\{(Bu_4N)(VO_2(C_2O_4))\}_n$ (II)**, **$[Pt(NH_3)_4][VO(H_2O)(C_2O_4)_2]\cdot 2H_2O$ (III)** and **$\{[Pt(NH_3)_4][VO(C_2O_4)_2]\}_n$ (IV).**

Complex	**$(Bu_4N)_2[VO(C_2O_4)_2]$ (I)**	**$\{(Bu_4N)(VO_2(C_2O_4))\}$ (II)**	**$[Pt(NH_3)_4][VO(H_2O)(C_2O_4)_2]\cdot 2H_2O$ (III)**	**$\{[Pt(NH_3)_4][VO(C_2O_4)_2]\}_n$ (IV)**
Empirical formula	$C_{36}H_{72}N_2O_9V$	$C_{18}H_{36}NO_6V$	$C_4H_{18}N_4O_{12}PtV$	$C_4H_{12}N_4O_9PtV$
Formula weight	727.89	413.42	560.25	506.21
Crystal system	monoclinic	monoclinic	triclinic	monoclinic
Space group, Z	C2/c, 4	$P2_1/n$, 4	P-1, 2	C2/c, 8
a(Å)	18.9092(19)	8.8694(5)	7.27950(10)	19.603(8)
b(Å)	13.9416(12)	14.9160(6)	8.24340(10)	7.945(3)
c(Å)	18.272(3)	16.6499(7)	12.9863(2)	15.358(6)
α/°	90	90	108.1350(10)	90
β/°	120.899(3)	103.309(2)	97.3040(10)	97.242(13)
γ/°	90	90	95.7430(10)	90
V(Å3)	4133.4(8)	2143.56(17)	726.455(18)	2372.8(16)
dCalc(g/cm3)	1.170	1.281	2.561	2.834
μ/mm^{-1}	0.289	0.493	10.331	12.618
F(000)	1588.0	888.0	534.0	1896.0
Crystal size (mm)	0.09 × 0.09 × 0.07	0.09 × 0.06 × 0.05	0.1 × 0.09 × 0.04	0.05 × 0.03 × 0.01
2Θ range for data collection/°	5.022– 56.558	4.81-54.978	3.348 - 66.264	5.348-46.522
Index ranges	-25 ≤ h ≤ 2 -18 ≤ k ≤ 18 -24 ≤ l ≤ 23	-11 ≤ h ≤ 11 -19 ≤ k ≤ 19 -20 ≤ l ≤ 21	-10 ≤ h ≤ 11 -12 ≤ k ≤ 12 -19 ≤ l ≤ 19	-21 ≤ h ≤ 21 -8 ≤ k ≤ 8 -17 ≤ l ≤ 10
Reflections collected	25901	23280	15497	4516
Independent reflections (*R*int)	5125 [R_{int} = 0.0738, R_{sigma} = 0.0543]	4914 [R_{int} = 0.0771, R_{sigma} = 0.0698]	5492 [R_{int} = 0.0258, R_{sigma} = 0.0279]	1703 [R_{int} = 0.1196, R_{sigma} = 0.1500]
Completeness to theta = 50.5°	99.9 %	99.8 %	100 %	99.8 %
Data / restraints / parameters	5125/0/222	4914/0/239	5492/0/213	1703/78/179
Goodness-of-fit on *F*2	1.040	1.035	1.065	0.950
Final *R* indices (I>=2σ (I))	R_1 = 0.0449, wR_2 = 0.1022	R_1 = 0.0473, wR_2 = 0.0951	R_1 = 0.0192, wR_2 = 0.0414	R_1 = 0.0561, wR_2 = 0.0987
R indices (all data)	R_1 = 0.0648, wR_2 = 0.1157	R_1 = 0.0729, wR_2 = 0.1098	R_1 = 0.0252, wR_2 = 0.0433	R_1 = 0.0996, wR_2 = 0.1190
Largest diff. peak and hole (e/Å3)	0.41/-0.32	0.32/-0.33	0.61/-1.58	1.33/-1.55

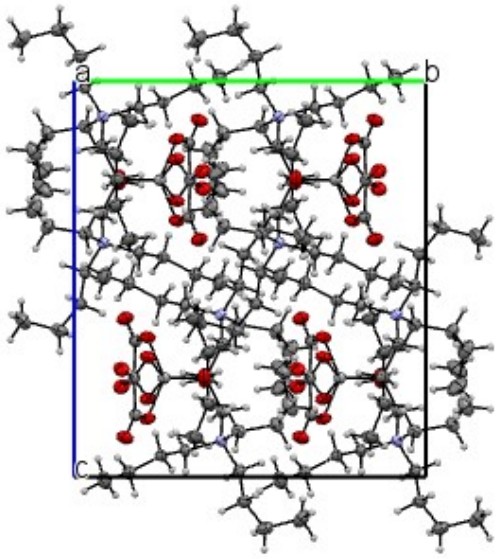

Figure S1. Packing of **$(Bu_4N)_2[VO(C_2O_4)_2]$ (I)** (view along the *a* axis).

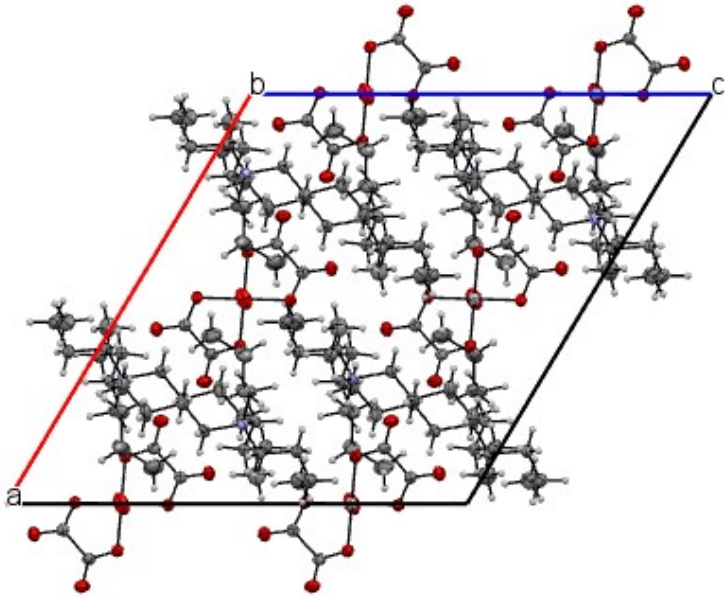

Figure S2. Packing of **$(Bu_4N)_2[VO(C_2O_4)_2]$ (I)** (view along the *b* axis).

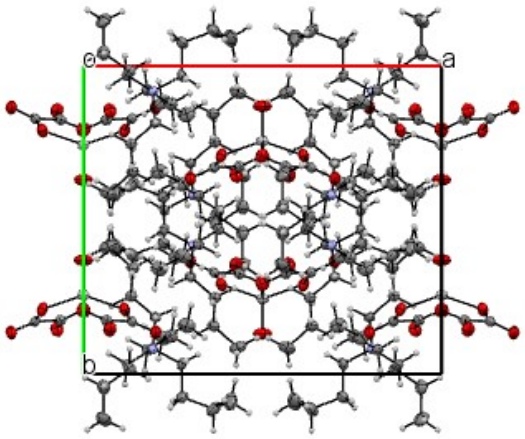

Figure S3. Packing of **$(Bu_4N)_2[VO(C_2O_4)_2]$ (I)** (view along the *c* axis).

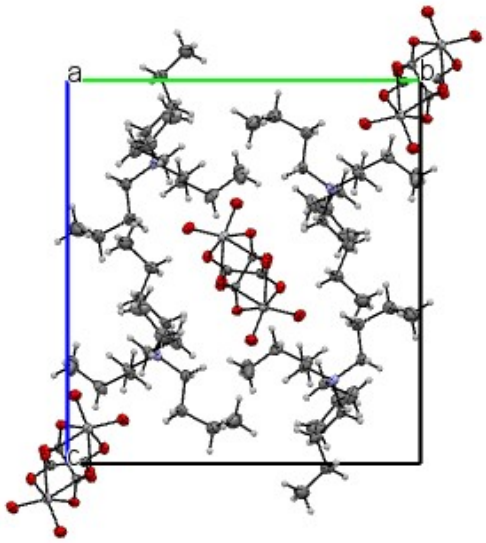

Figure S4. Packing of **{(Bu$_4$N)(VO$_2$(C$_2$O$_4$))}$_n$ (II)** (view along the *a* axis).

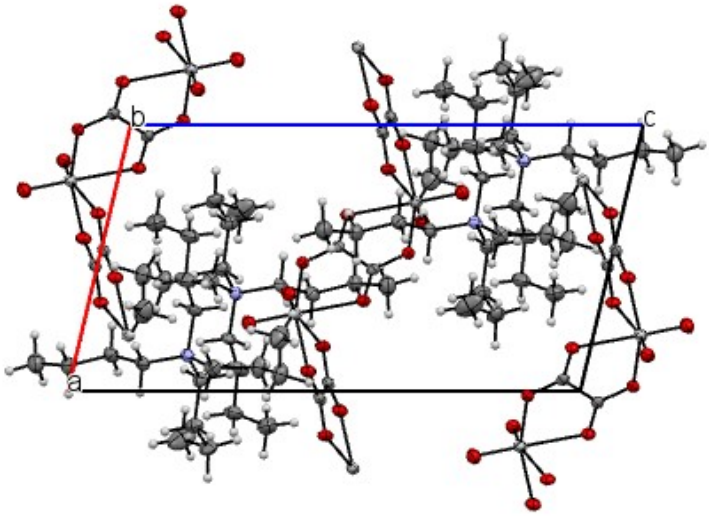

Figure S5. Packing of **{(Bu$_4$N)(VO$_2$(C$_2$O$_4$))}$_n$ (II)** (view along the *b* axis).

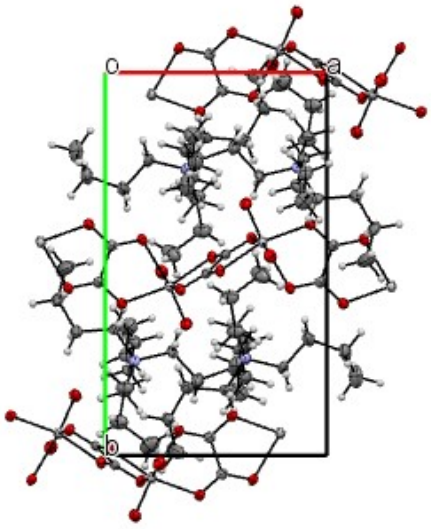

Figure S6. Packing of **{(Bu$_4$N)(VO$_2$(C$_2$O$_4$))}$_n$ (II)** (view along the *c* axis).

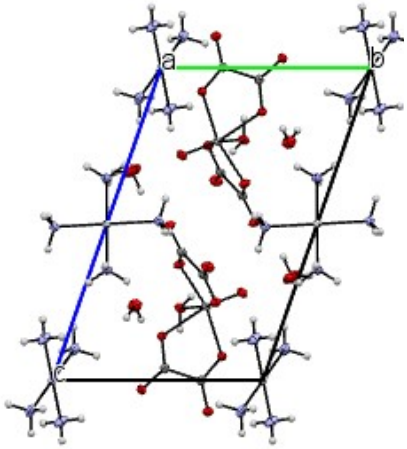

Figure S7. Packing of **$[Pt(NH_3)_4][VO(H_2O)(C_2O_4)_2]\cdot 2H_2O$ (III)** (view along the *a* axis).

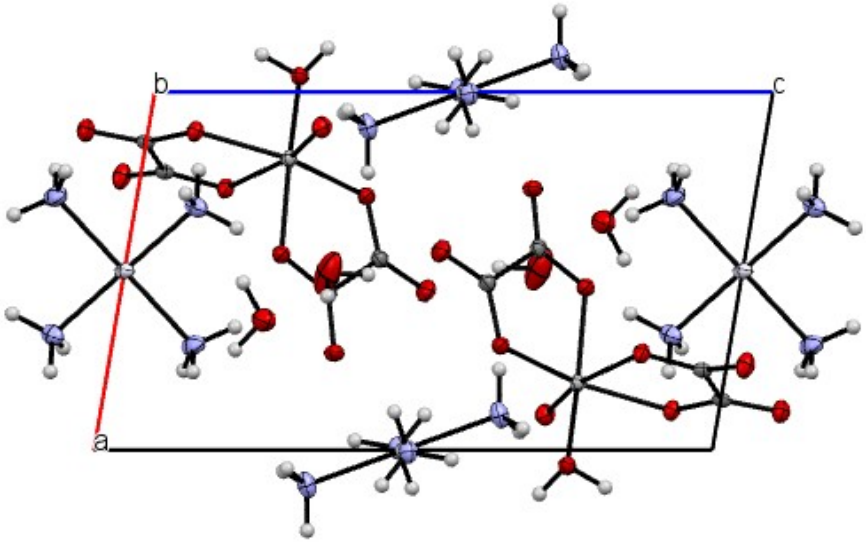

Figure S8. Packing of **$[Pt(NH_3)_4][VO(H_2O)(C_2O_4)_2]\cdot 2H_2O$ (III)** (view along the *b* axis).

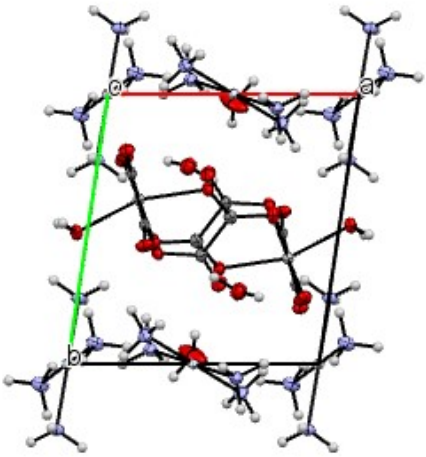

Figure S9. Packing of **$[Pt(NH_3)_4][VO(H_2O)(C_2O_4)_2]\cdot 2H_2O$ (III)** (view along the *c* axis).

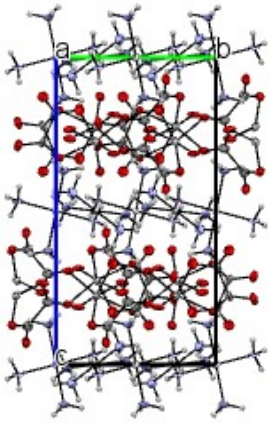

Figure S10. Packing of **{[Pt(NH$_3$)$_4$][VO(C$_2$O$_4$)$_2$]}$_n$ (IV)** (view along the *a* axis).

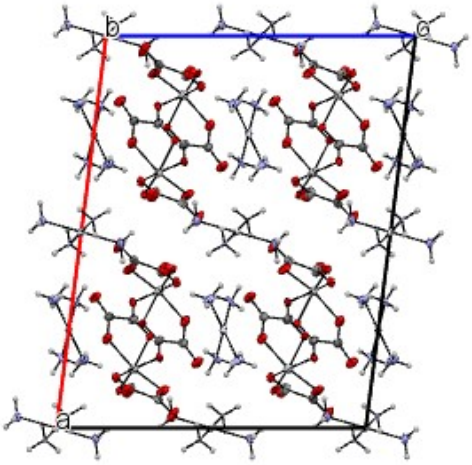

Figure S11. Packing of **{[Pt(NH$_3$)$_4$][VO(C$_2$O$_4$)$_2$]}$_n$ (IV)** (view along the *b* axis).

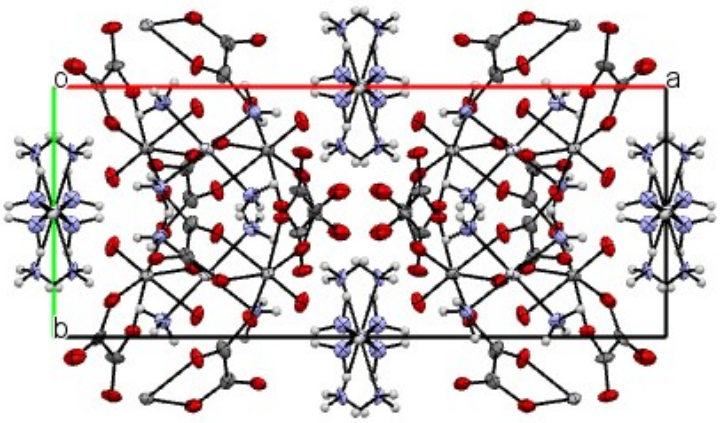

Figure S12. Packing of **{[Pt(NH$_3$)$_4$][VO(C$_2$O$_4$)$_2$]}$_n$ (IV)** (view along the *c* axis).

IR spectra

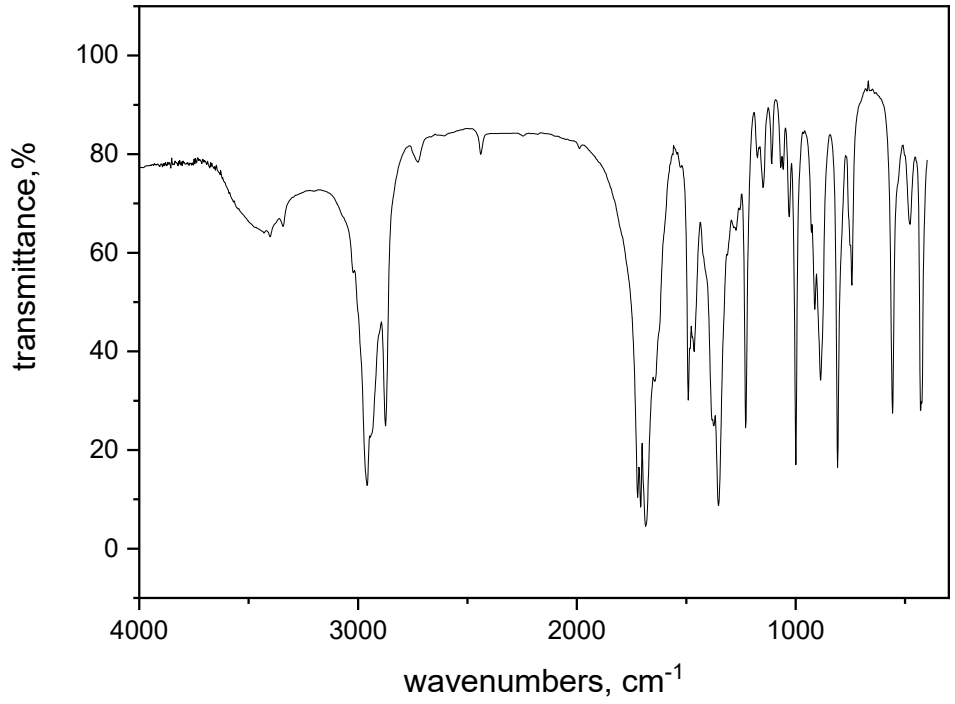

Figure S13. IR spectrum of **$(Bu_4N)_2[VO(C_2O_4)_2]$ (I).**

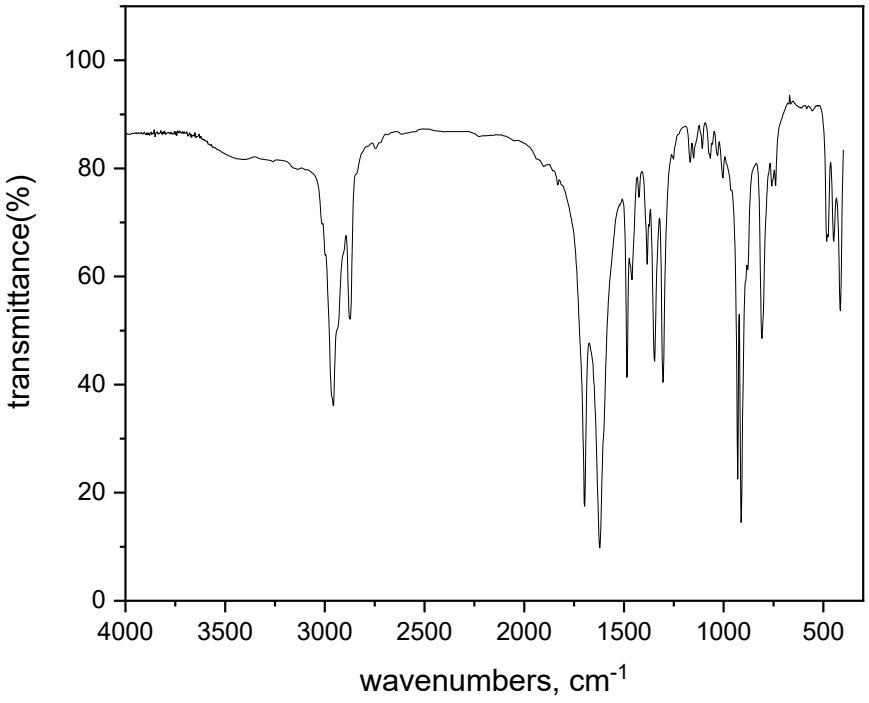

Figure S14. IR spectrum of **$\{(Bu_4N)(VO_2(C_2O_4))\}_n$(II).**

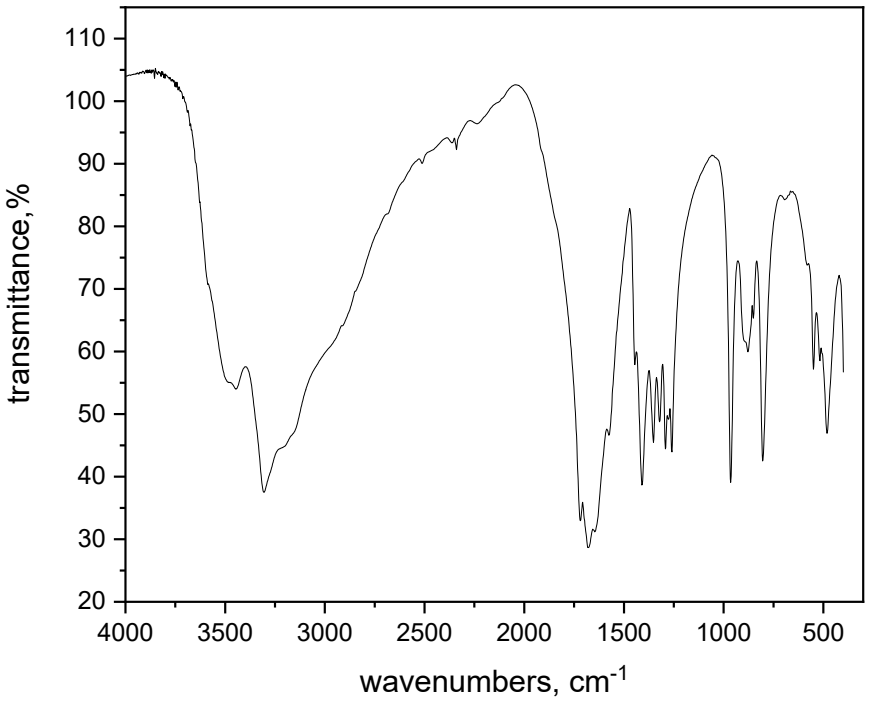

Figure S15. IR spectrum of **$[Pt(NH_3)_4][VO(H_2O)(C_2O_4)_2]\cdot 2H_2O$(III).**

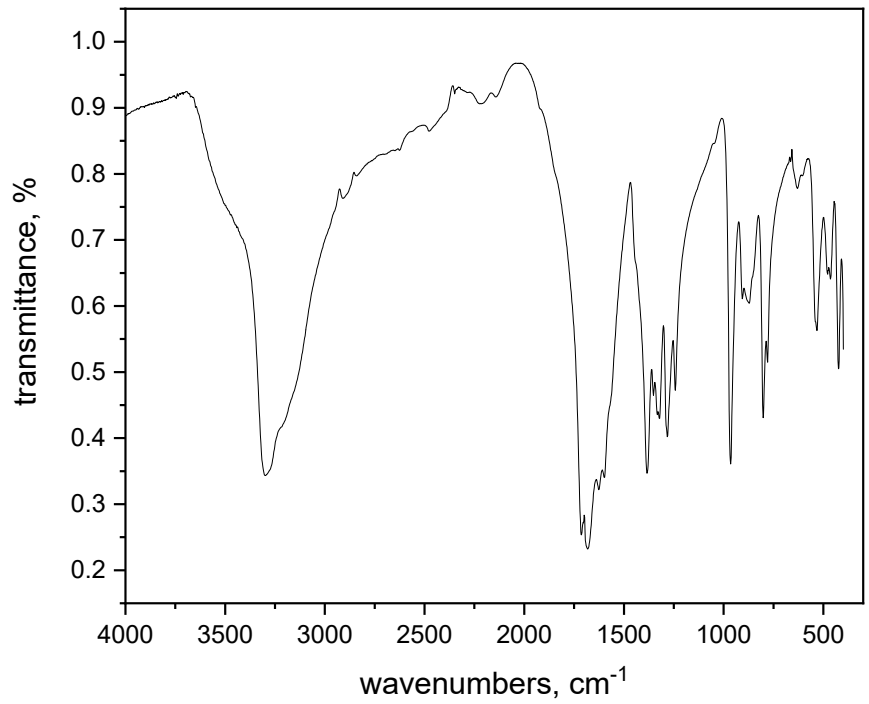

Figure S16. IR spectrum of **$\{[Pt(NH_3)_4][VO(C_2O_4)_2]\}_n$ (IV).**

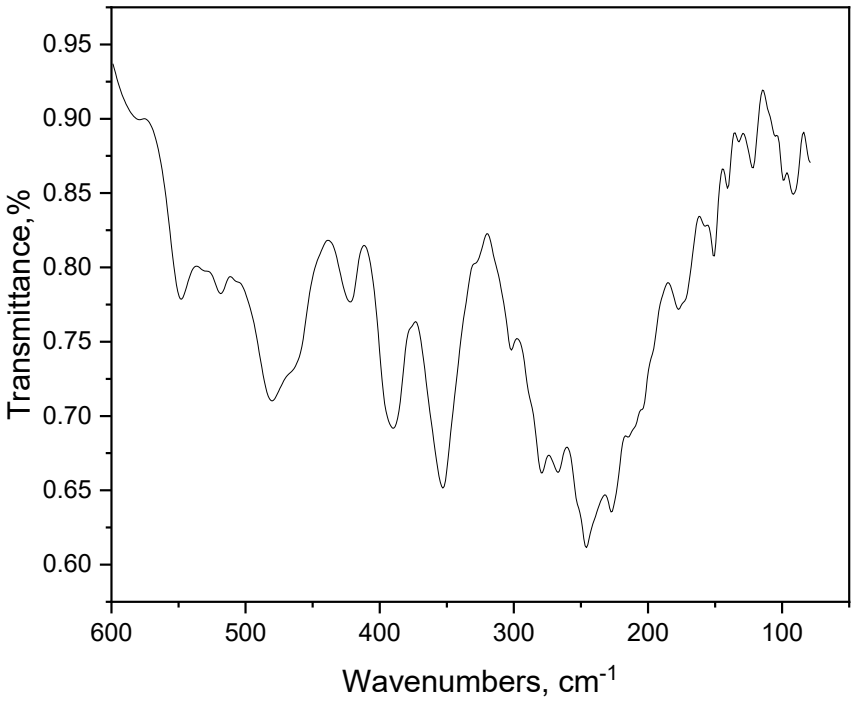

Figure S17. IR spectrum of **$[Pt(NH_3)_4][VO(H_2O)(C_2O_4)_2]\cdot 2H_2O$(III).**

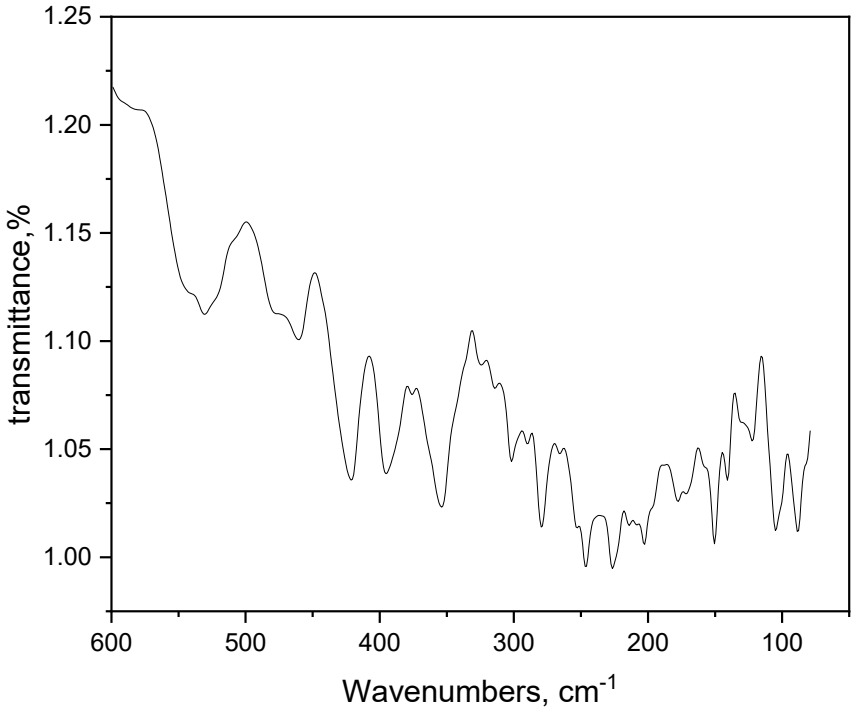

Figure S18. IR spectrum of **$\{[Pt(NH_3)_4][VO(C_2O_4)_2]\}_n$ (IV).**

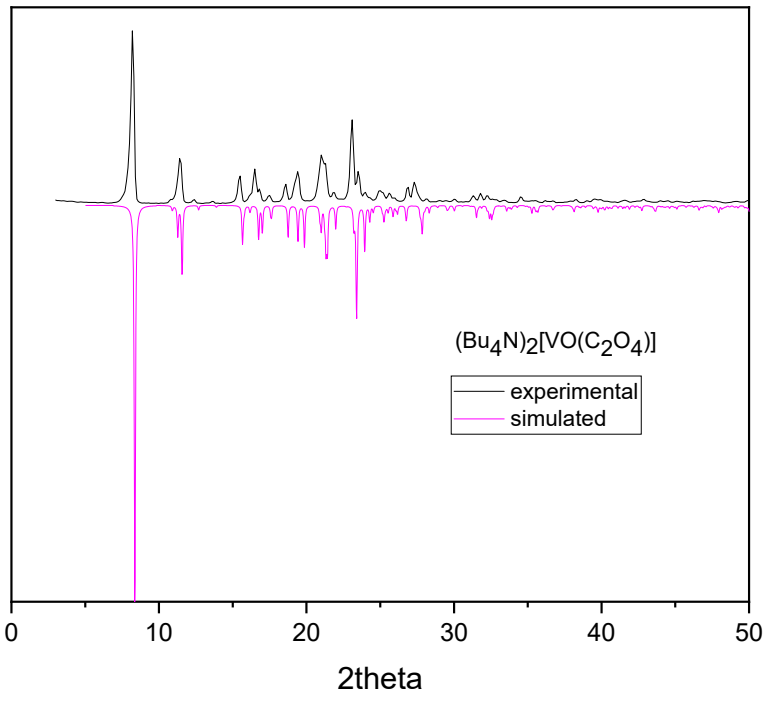

Figure S19. X-ray powder diffraction pattern of **$(Bu_4N)_2[VO(C_2O_4)_2]$(I)**.

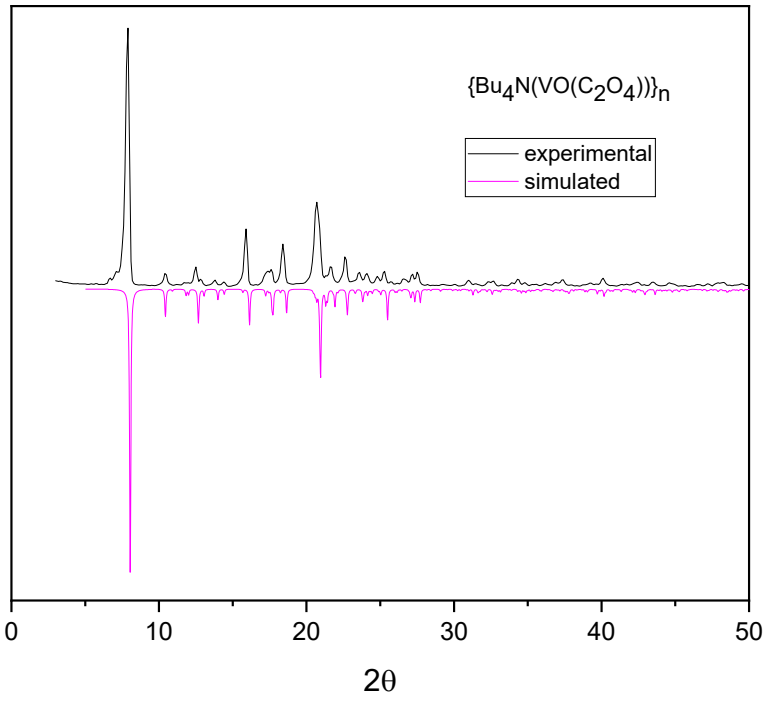

Figure S20. X-ray powder diffraction pattern of **$\{(Bu_4N)(VO_2(C_2O_4))\}_n$(II)**.

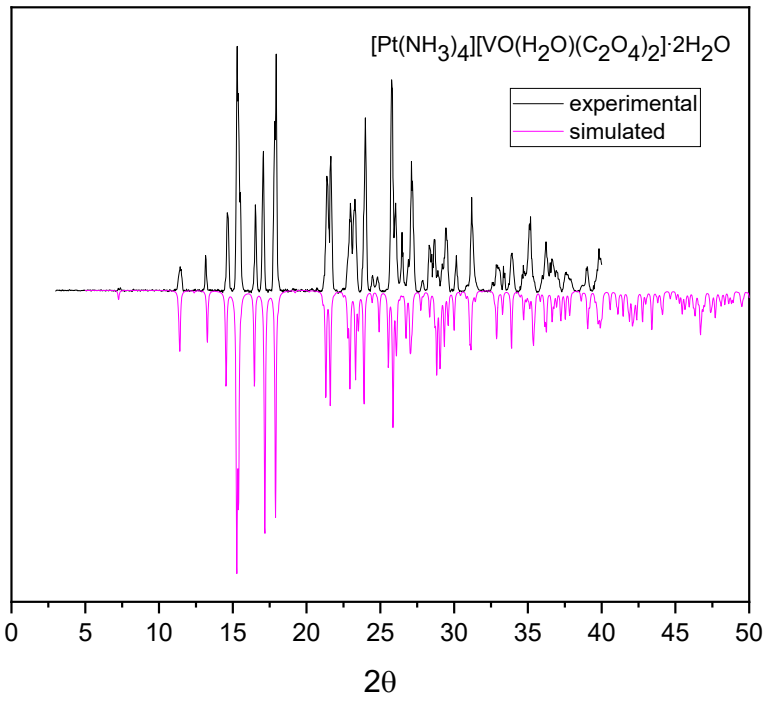

Figure S21. X-ray powder diffraction pattern of **$[Pt(NH_3)_4][VO(H_2O)(C_2O_4)_2]\cdot 2H_2O$(III)**.

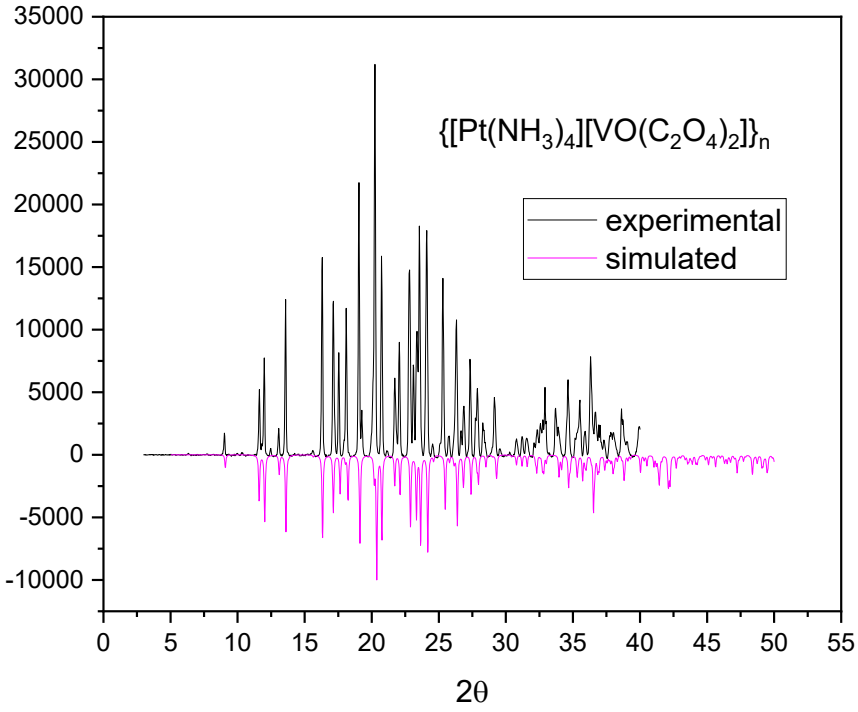

Figure S22. X-ray powder diffraction pattern of **$\{[Pt(NH_3)_4][VO(C_2O_4)_2]\}_n$ (IV).**

EPR

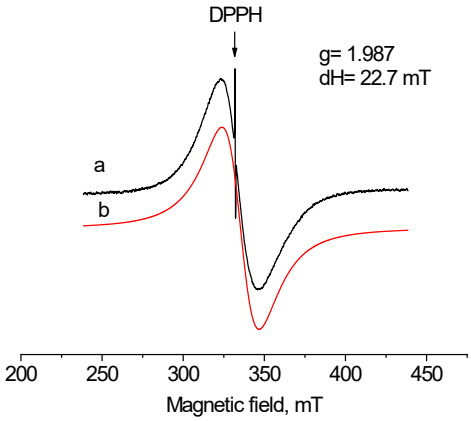

Figure S23. EPR spectra of **{[Pt(NH$_3$)$_4$][VO(C$_2$O$_4$)$_2$]}$_n$ (IV):** a- experimental, b- simulated.

TG

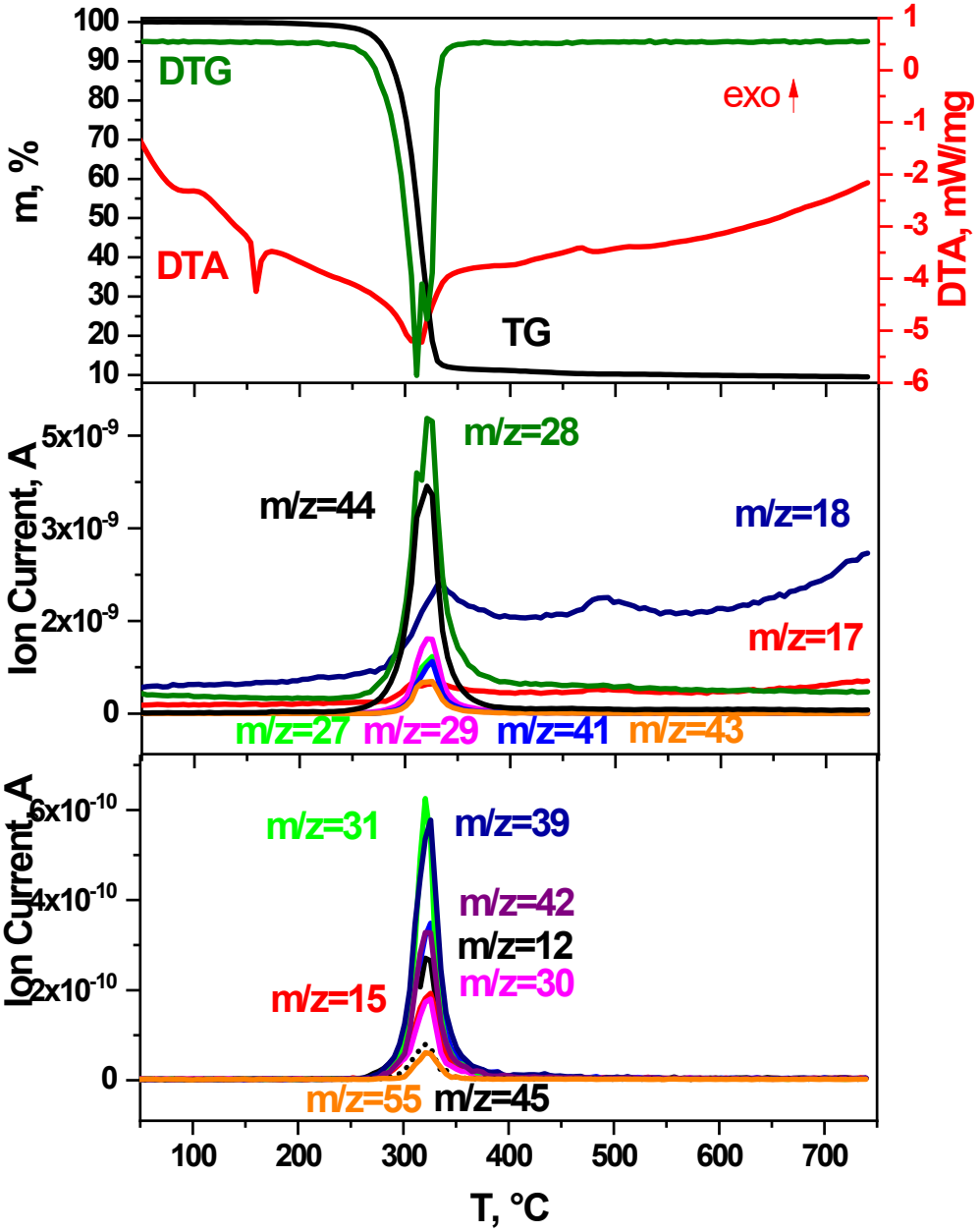

Figure S24. TG curves of **$(Bu_4N)_2[VO(C_2O_4)_2]$(I)** obtained in reducing atmosphere at a heating rate of 10 deg/min.

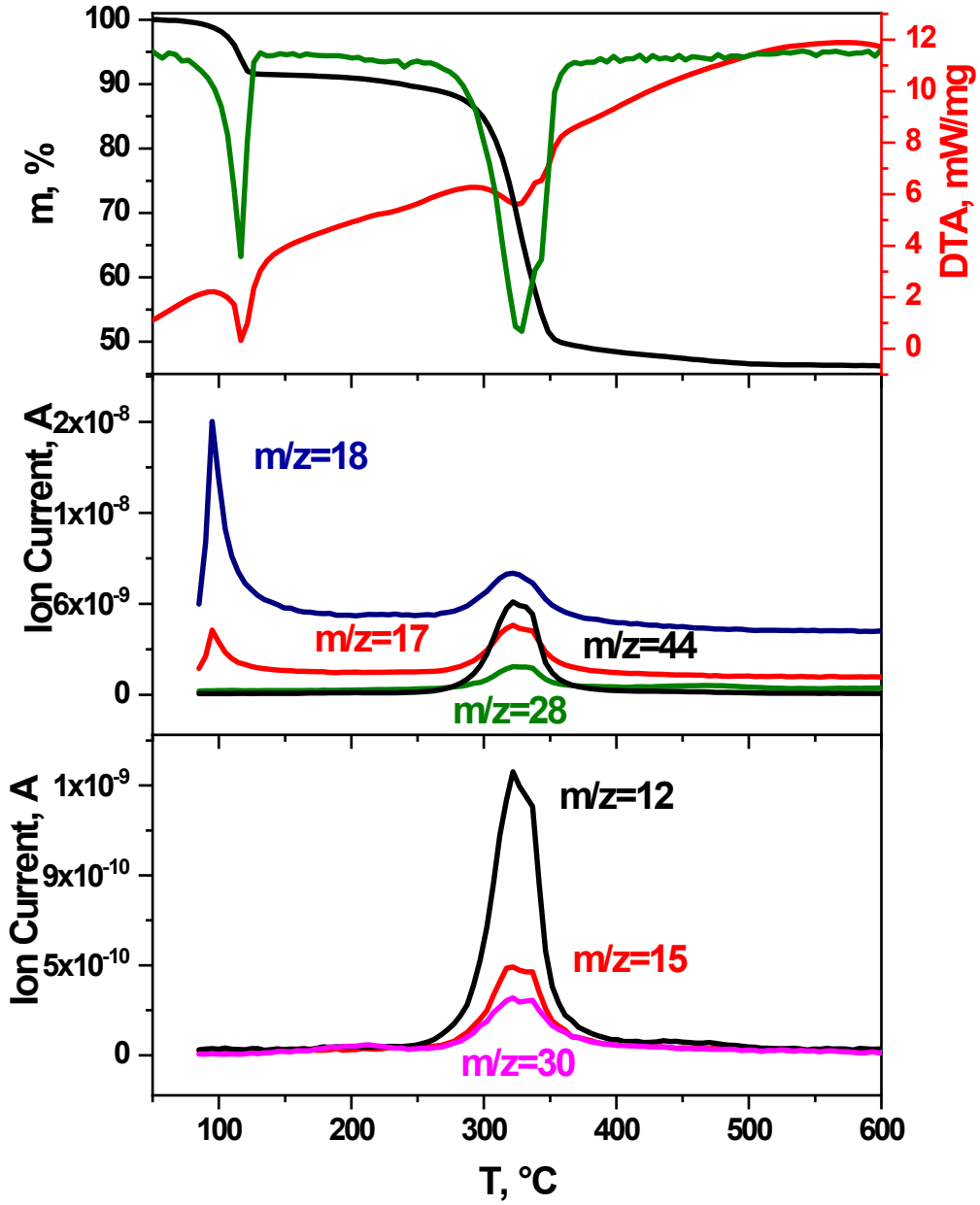

Figure S25. TG curves of **$[Pt(NH_3)_4][VO(H_2O)(C_2O_4)_2]\cdot 2H_2O$(III)** obtained in inert (He) atmosphere at a heating rate of 10 deg/min.

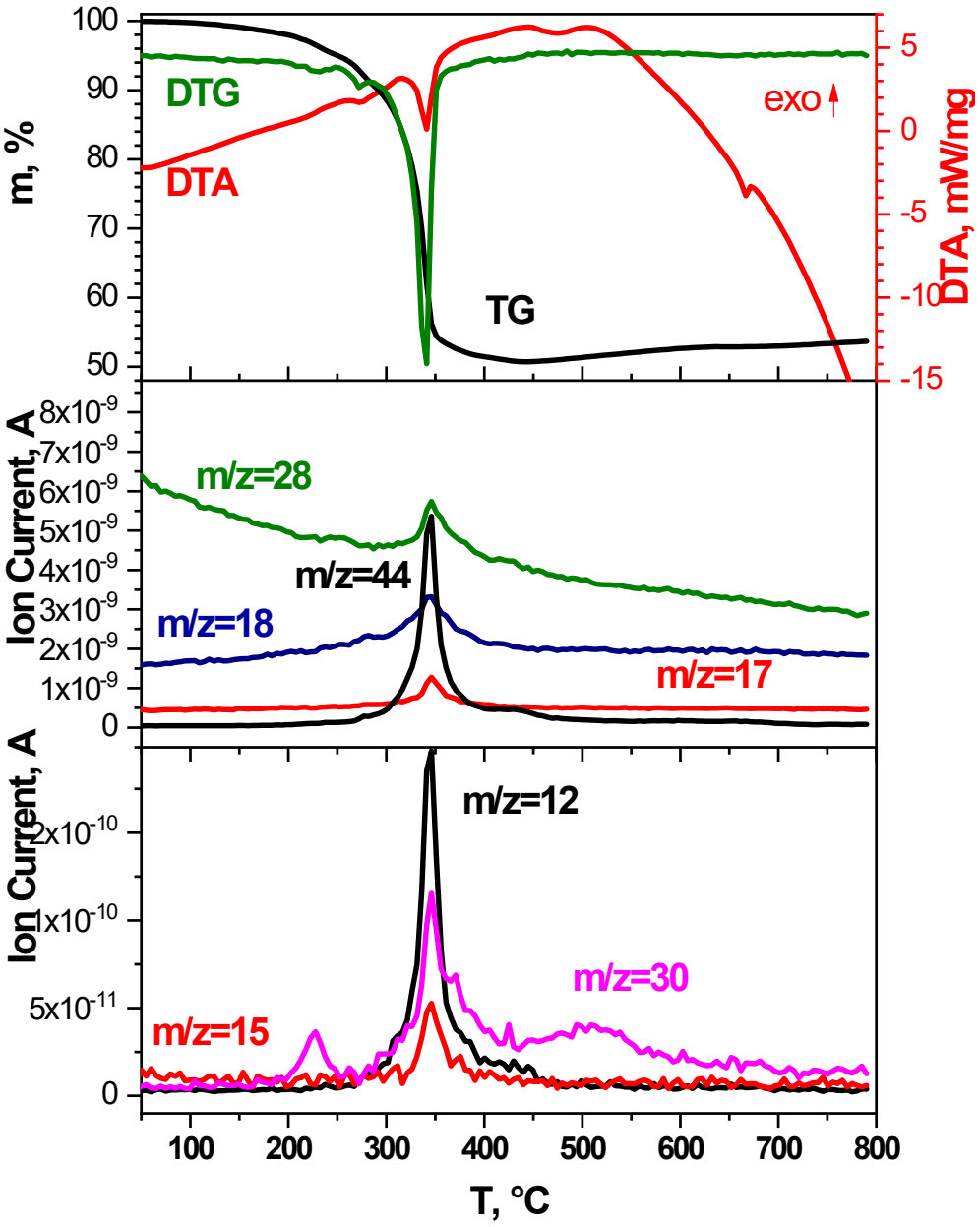

Figure S26. TG curves of **{[Pt(NH$_3$)$_4$][VO(C$_2$O$_4$)$_2$]}$_n$ (IV)** obtained in inert atmosphere at a heating rate of 10 deg/min.

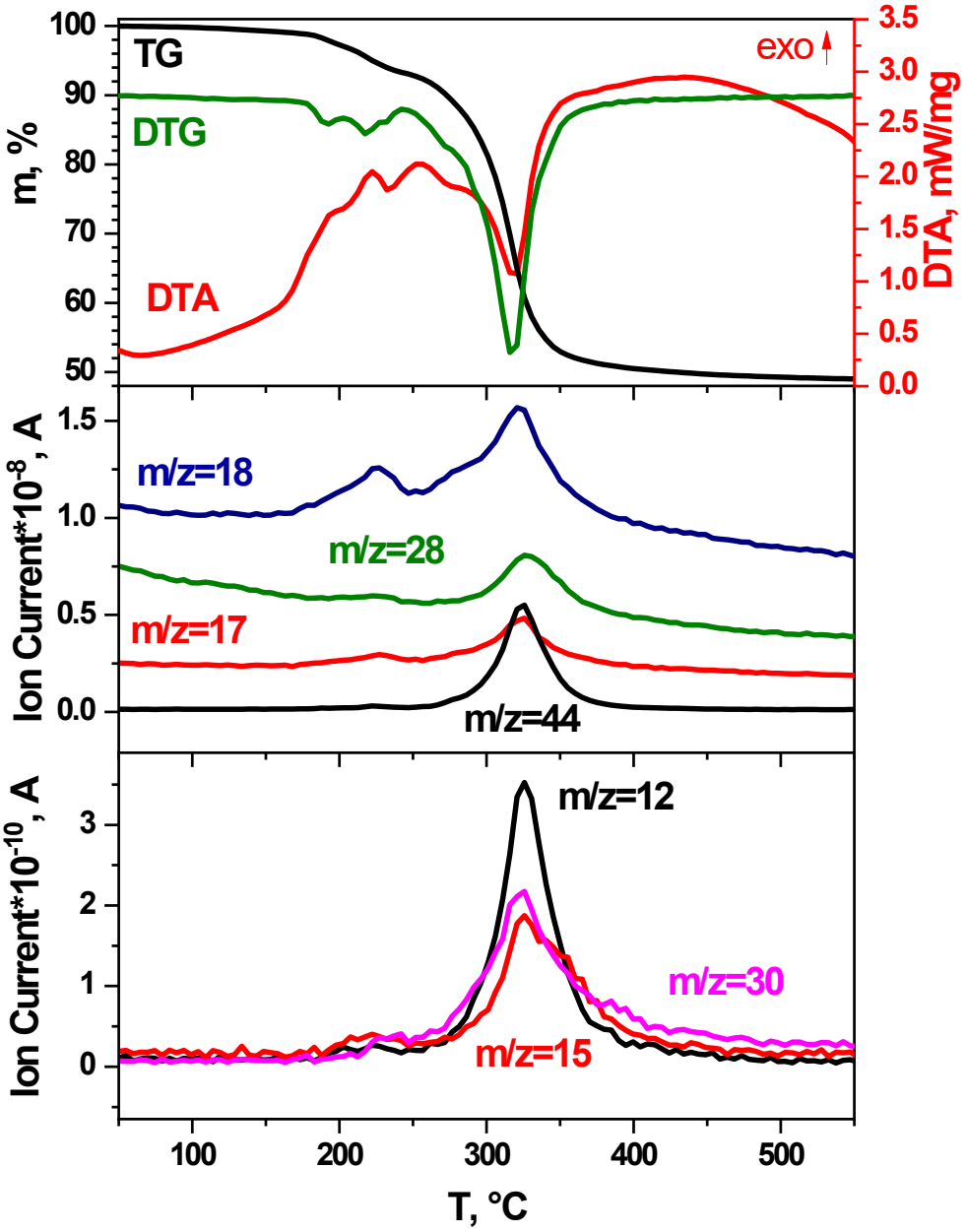

Figure S27. TG curves of of **{[Pt(NH$_3$)$_4$][VO(C$_2$O$_4$)$_2$]}$_n$ (IV)** obtained in reducing atmosphere at a heating rate of 10 deg/min.

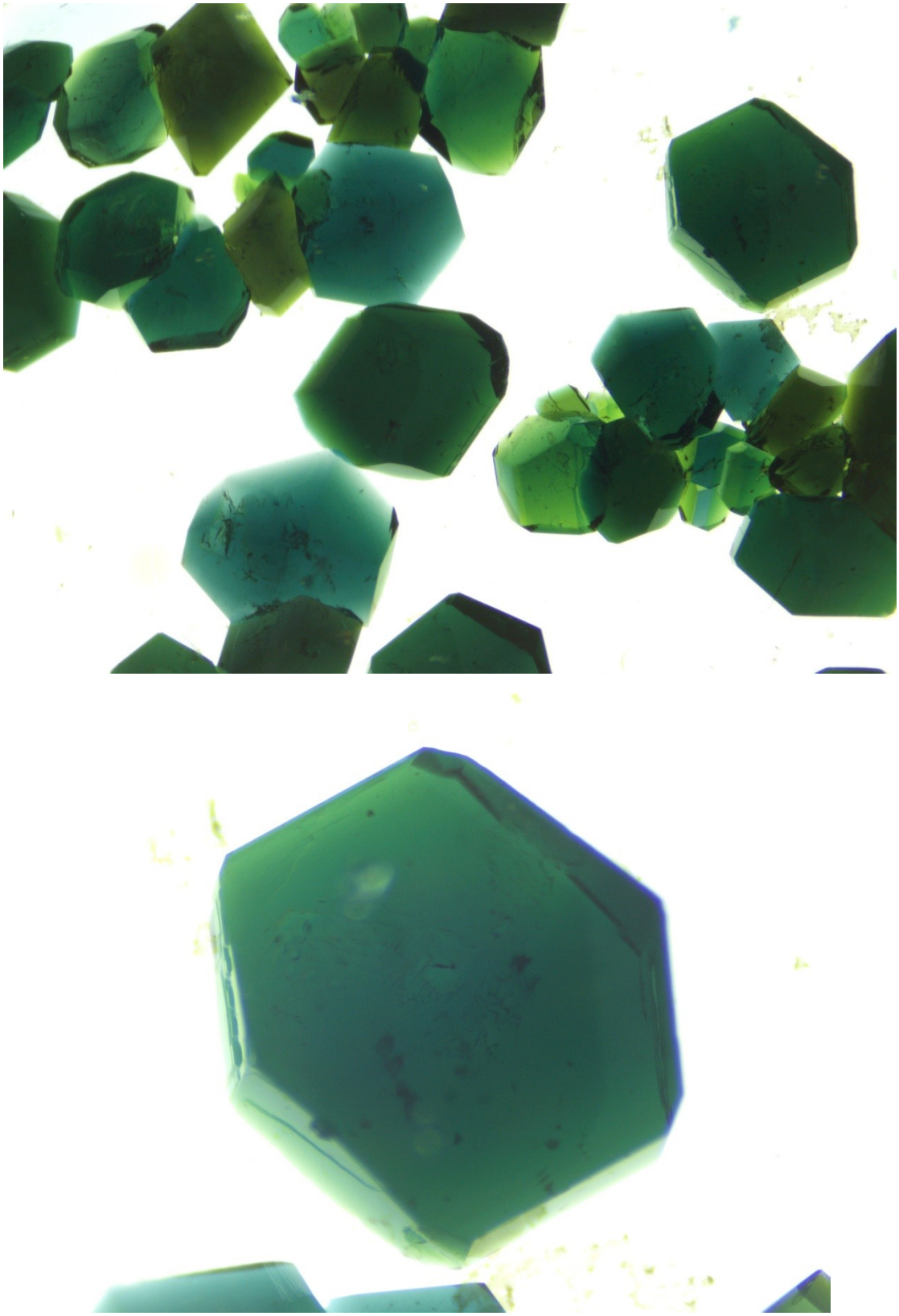

Figure S28. Microscope image of **$(Bu_4N)_2[VO(C_2O_4)_2]$(I).**

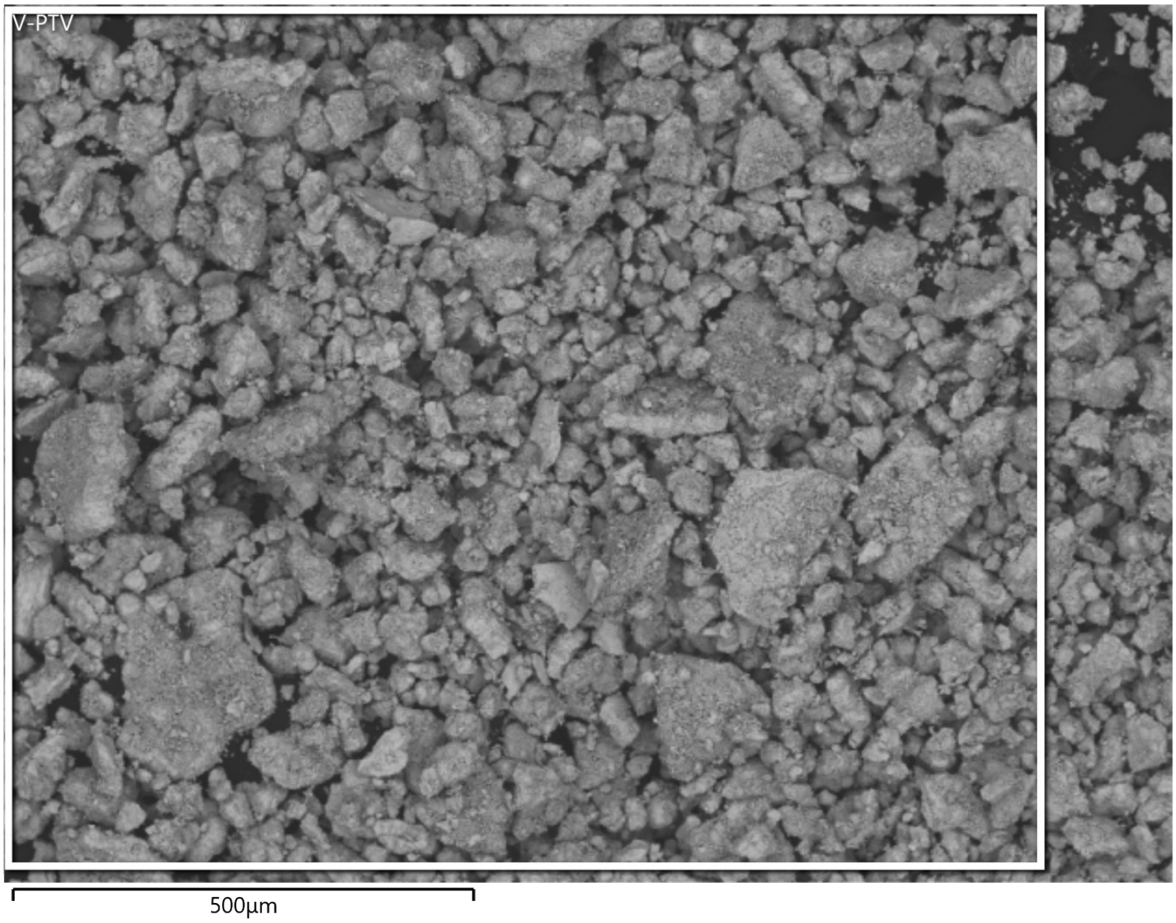

Figure S29. SEM pictures of **IV** thermolysis product at 700°C for 1 hour at two different scales**.**